JCSE The Journal of Corrosion Science and Engineering
ISSN 1466-8858 Volume 14, Preprint 43 submitted 6 December 2011

Susceptibility of Pipeline Girth Welds to Hydrogen Embrittlement and Sulphide Stress Corrosion Cracking.

Adriana Forero Ballesteros[1], José A. da Cunha Ponciano[2], Ivani de S. Bott[1]
[1] Pontifical Catholic University of Rio de Janeiro, – Materials Engineering Department, Rua Marquês de São Vicente, 225, Gávea Rio de Janeiro, RJ - Brazil - 22453-900 Cx. Postal: 38097 phone fax: (5521) 3527-1253. [2]COPPE, Department of Metallurgical and Materials Engineering, Corrosion Laboratory, Ilha do Fundão, IF-B, telephone Tel: (5521)2290-1448 / 2290-1544 / 2290-1615
adriafob@hotmail.com, ponciano@metalmat.ufrj.br, bott@puc-rio.br

Abstract

The susceptibility of girth welds to Sulphide Stress Corrosion Cracking (SSCC) and Hydrogen Embrittlement (HE) were evaluated for API grade X80 and X56 steels, both for similar (X80/X80) and dissimilar (X80/X56) joints. Slow strain rate (SSR) and Hydrogen Permeation tests were performed at room temperature using sodium thiosulphate solutions at different pH levels. The SSR tests showed that the majority of the welded joints studied, though approved by the API 1104 standard´s criteria, did in fact suffer a reduction in ductility and showed indications of susceptibility to sulphide stress corrosion cracking and to hydrogen embrittlement in the form of secondary longitudinal and internal transverse cracks. This was true regardless the welding process used.

Keywords: HSLA, HE, SSCC, Corrosion, Welding.

1. Introduction

The increasing demand for transport of gas, oil and derivatives under severe service conditions over recent decades has generated major challenges regarding the specification of materials for the manufacture of pipelines. The global trends for this sector of the petroleum industry, point to the use of pipes with larger diameters and smaller wall thicknesses, operating under high pressure. A full understanding of the behaviour of these steel pipes at all stages is essential; from the design project and the fabrication and construction of the pipelines, to their operation in different environments. This knowledge must then be applied to ensure the long term structural integrity of the pipelines, which is of fundamental importance to the oil and gas industry. The steel pipes are manufactured using low carbon steels with microalloying additions of Nb, Ti and V to obtain the necessary levels of strength, toughness and weldability [1-6]. Additionally, steel pipelines are often exposed to conditions that can potentially lead to Hydrogen Induced Cracking (HIC) and Sulphide Stress Corrosion Cracking (SSCC).

The susceptibility of pipeline steels to sulphide stress corrosion cracking (SSCC) and hydrogen embrittlement (HE) depends on a series of factors ranging from those associated with the manufacture of the steel, the pipe fabrication and the assembly of the pipeline, to those associated with the type of substances to be transported. It has been acknowledged [7-16] that welding can increase susceptibility of these steels to SSCC and hydrogen embrittlement due to the metallurgical changes and residual stresses introduced by the procedures involved. However, the exact corrosion mechanism active at the welded joints steel has remained unclear [17-21].

ASTM G129-00 Slow Strain Rate (SSR) tensile testing [22] in sodium thiosulphate solutions at different (acidic) pH levels and Hydrogen Permeation tests were used to study the susceptibility of similar (X80/X80) and dissimilar (X80/X56) girth welds to Sulphide Stress Corrosion Cracking (SSCC) and Hydrogen Embrittlement (HE). The greatest losses in ductility and the highest hydrogen permeation current densities were found for the solutions with lowest pH levels. The base metal microstructure (Ferrite and

microconstituent MA - martensite and austenite) was the most susceptible according to the SSR test results. These results were consistent with the hydrogen permeation test results. It was also found that transgranular fracture was the most common fracture mechanism.

2. Experimental Procedure

2.1 Materials

Girth welded pipes, produced in accordance with specifications required by the API 5L Standard [23], were investigated. Full circumference welded joint ring samples were obtained from tube sections of API 5L X80 and X56 steels. The tubes were fabricated using the UOE process from a steel sheet produced by a thermomechanical controlled process (TMCP) without accelerated cooling. Three different processes, Shielded metal arc welding (SMAW), Flux-cored arc welding - Gas Shielded (FCAW-G), Gas metal arc welding -Surface Tension Transfer (GMAW- STT) were used, applying four different welding procedure specifications (WPS) (Table 1).

Table 1. Overview of welding procedures used.

Joint	Materials	Processes	Consumables		
			Root pass	Hot pass	Filling pass and top bead
X80-1	X80–X80	SMAW	E 6010	E 8018-G	E 10018-G
X80-2	X80–X56	SMAW	E 6010	E 8018-G	E 10018-G
X80-3	X80–X80	SMAW FCAW-G	E 6010	E8010-P1	E 101T1-GM-H8
X80-4	X80–X80	GMAW (STT) + FCAW-G	ER 80S-G	E101 T1-GM-H8	E 101T1-GM-H8

The chemical compositions of the base and weld metals are shown in Table 2. Mechanical properties of X80 and X56 base metal and the average values of the mechanical properties of welded joints are shown in Table 3. The hardness profile (Figure 1) for the different areas of the welded joint (base metal, heat affected zone and weld metal) was calculated according to NACE Standard MR0-175 [24], by averaging the results obtained of several specimens.

Table 2. Chemical Compositions of the base metal and welded joints (wt%)

Material	C	Si	Mn	P	S	Cr	Ni	Mo	Ti	V	Nb
Base Metal X80	0.072	0.152	1.84	0.017	0.007	0.171	0.025	0.200	0.013	0.020	0.061
Base Metal X56	0.099	0.207	1.49	0.020	0.007	0.031	0.018	0.009	0.013	0.002	0.045
Joint X80-1	0.091	0.340	1.46	0.014	0.012	0.062	1.020	0.048	0.012	0.010	0.063
Joint X80-2	0.091	0.420	1.58	0.015	0.012	0.045	1.030	0.022	0.013	0.011	<0.003
Joint X80-3	0.087	0.276	1.46	0.011	0.010	0.061	0.440	0.223	0.020	0.014	0.011
Joint X80-4	0.078	0.370	1.65	0.012	0.012	0.052	0.470	0.306	0.072	0.014	0.009

Table 3. Mechanical properties of the base metals and the joints of API 5L-X80 steel pipe.

Material	σ_{YS} (Mpa)	UTS (MPa)	Elongation %
Base Metal X80	602	682	30.9
Base Metal X56	456	557	30.4
Joint X80-1	612	673	22.3
Joint X80-2	486	564	23.6
Joint X80-3	611	670	25.3
Joint X80-4	633	683	23.8

JCSE The Journal of Corrosion Science and Engineering
ISSN 1466-8858 Volume 14, Preprint 43 submitted 6 December 2011

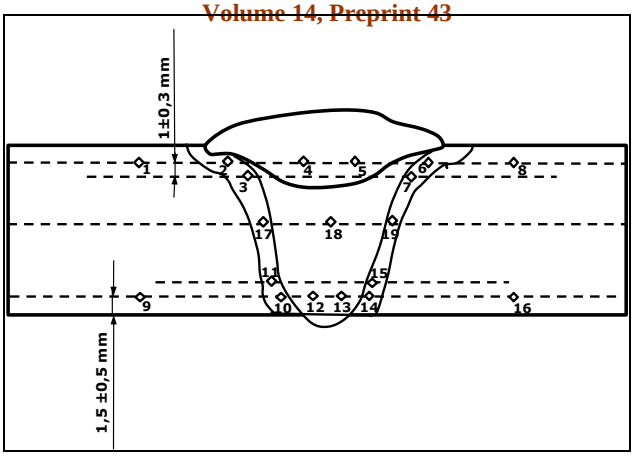

Figure 1.Hardness profile determined according to NACE Standard TM0-175.

Samples for microstructural analysis were prepared using the conventional method of grinding (from 220 to 1200 grades) and diamond paste semi-automatic polishing from 6 to 3 µm. Microstructural analysis was performed using optical microscopy (OM), on samples etched in 2% Nital solution for 5 to 10 seconds. For Scanning Electron Microscopy (SEM), an electrolytic double etching technique was used to adequately reveal the presence of constituent MA. The procedure was performed as follows: first electrolytic etch: 5g EDTA, 0.5g NaF and 100 ml of distilled water, at 5V for 15 seconds, second electrolytic etch: 5g picric acid, 25 g NaOH and 100 ml of distilled water, at 5V for 100 seconds.

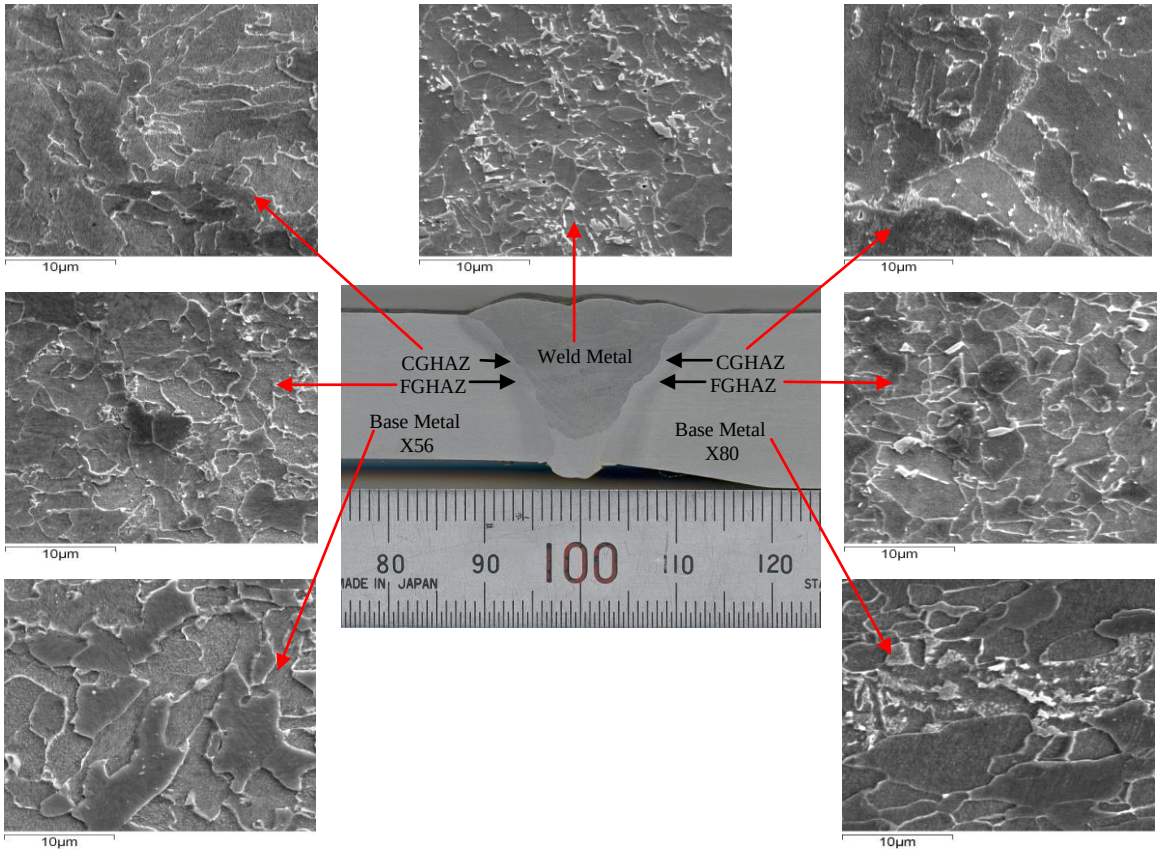

Figure 2. Microstructural Characterization of welded joint X80- 2.

JCSE The Journal of Corrosion Science and Engineering
ISSN 1466-8858 Volume 14, Preprint 43 submitted 6 December 2011

The general microstructural characterization of welded joints X80-2 and X80-3 is presented in Figures 2 and 3 respectively. The X80 base metal exhibited a ferritic structure with MA microconstituent, while the X56 base metal was basically ferrite and pearlite. The weld metal microstructure was mainly acicular ferrite and grain boundary ferrite. The HAZ of the X80 steel exhibited an lower bainite structure with decomposed MA microconstituent.

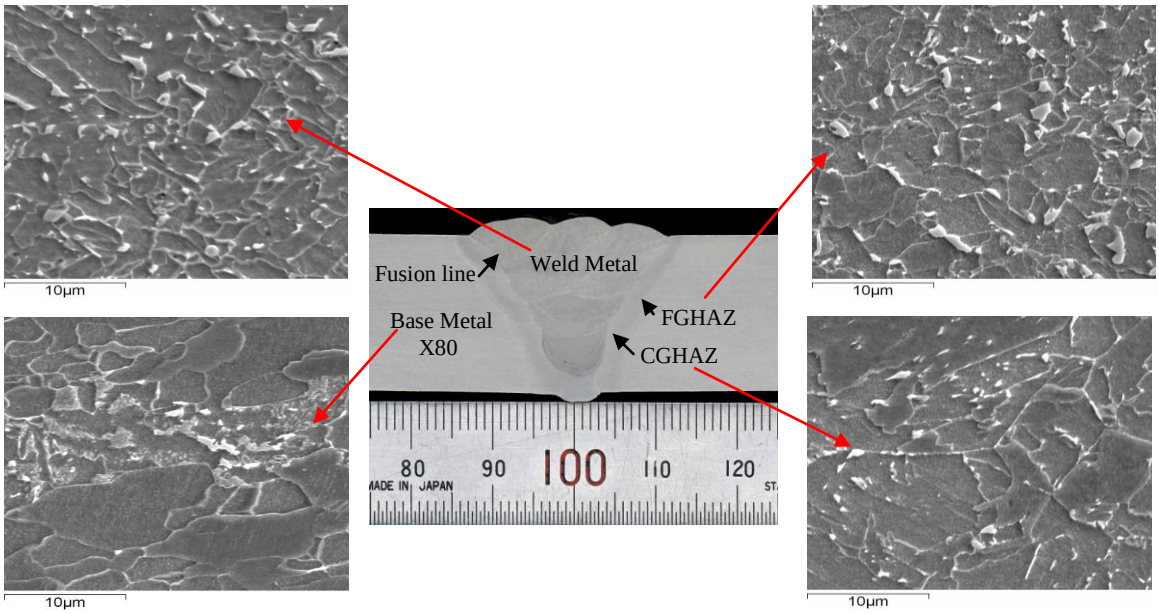

Figure 3. Microstructural Characterization of welded joint X80-3.

2.2. Slow Strain Rate Tests

Slow strain rate tensile tests (SSRT) were performed according to the ASTM G 129-00 standard, in air and in a test solution at 25°C, under axial loading at a strain rate of 2.8 $x10^{-5}s^{-1}$. Different corrosive environments based on a sodium thiosulphate solution were used (Table 4), where H_2S was generated indirectly by the reaction of the solution in contact with the metal surface [9]. The size and geometry of the specimens used in the tests are shown in Figure 4. Special care was taken to ensure that the circumferential weld seam was located in the centre of the gage length.

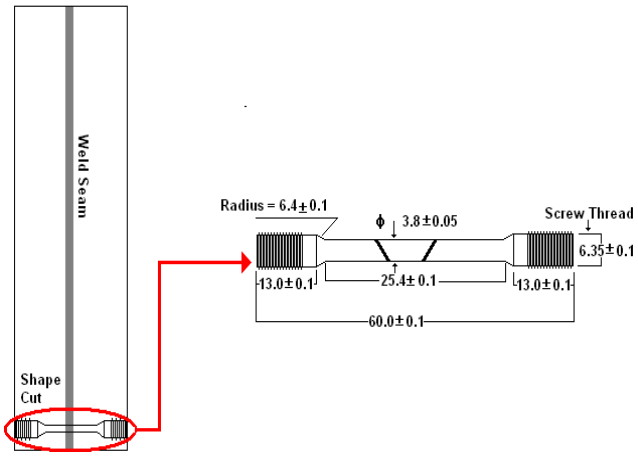

Figure 4. Schematic diagram of SSR specimen. Dimensions in mm.

OM and SEM were used to evaluate the topographical aspects of the fracture surfaces of the SSR specimens, and also to investigate crack propagation modes. Samples were cut from the tested specimens, both from the gage length, and at the fracture surface, and were mounted in bakelite. Microstructural analysis was carried out in two conditions; polished and etched.

2.3 Hydrogen Permeation Tests

The electrochemical hydrogen permeation tests were carried out using a Devanathan–Stachurski two-component cell, separated by the sample as working electrode. The specimens were cut by electro-erosion in order to obtain a final thickness of 3 mm, and the working area was 0.76 cm^2. Prior to the tests, all the specimens were ground to 600-grade emery paper, and cleaned with distilled water and methanol. The hydrogen exit cell was filled with 1M NaOH solution, which covered the entire surface of the working electrode. The hydrogen charging solutions are identified as solutions 1 to 4 (Table 4).

Table 4. Chemical compositions of the SSR test solutions.

Components	Sodium Thiosulphate $Na_2S_2O_3$	Sodium Chloride NaCl	Acetic Acid CH_3COOH	pH
Solution 1	10^{-3} mol/l	5%	0.50%	3.4
Solution 2	10^{-3} mol/l	5%	0.50%	4.4
Solution 3	10^{-4} mol/l	5%	0.50%	3.4
Solution 4	10^{-4} mol/l	5%	0.50%	4.4

The surface of the specimen facing the hydrogen charging side was maintained in an open circuit state. The detection cell included a saturated calomel reference electrode (SCE) and a platinum wire as counter electrode. The hydrogen permeation current was measured by anodically polarizing on the detection side of the working electrode (specimen) at +100mV as is shown schematically in Figure 5.

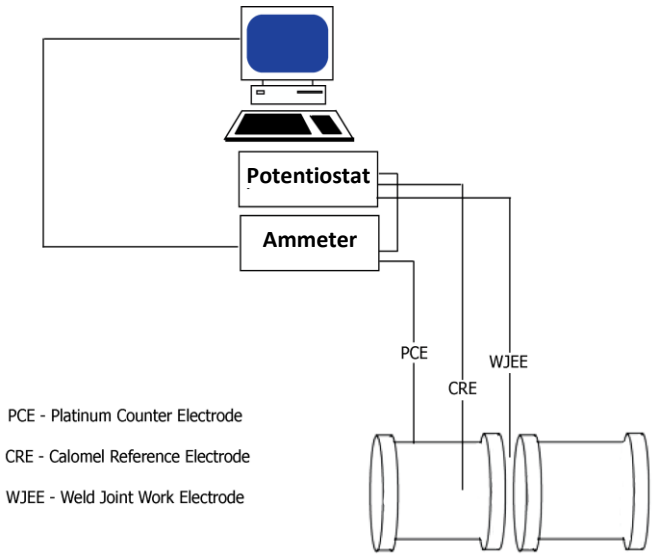

Figure 5. Experimental arrangement of hydrogen permeation tests.

JCSE The Journal of Corrosion Science and Engineering
ISSN 1466-8858 Volume 14, Preprint 43 submitted 6 December 2011

3. Results and Discussion

3.1. Slow Strain Rate Tests

The majority of specimens tested in the different sodium thiosulphate solutions exhibited considerable loss of ductility when compared with those tested in air. A higher average strain (16.4%) and lower average value of tensile strength (280MPa) were observed for samples tested in air (Figure 6) as compared with the results for samples tested in solution, the latter having presented an average strain of 12.07% and average tensile strength of 344 MPa, thus confirming the loss of ductility for the samples exposed to the test solutions.

According to "ASTM G129-00", the susceptibility of the materials to sulphide stress corrosion cracking and hydrogen embrittlement in SSRT tests can be evaluated by the ratio between the reductions in area when tested in air and when tested in a corrosive environment and according to equation (1).

$$RRA = RA_a/RA_c \quad \textbf{(1)}$$

Where RRA is the ratio of reduction in area, and RA_a e RA_c are the reductions in area after fracture for the specimen tested in air and in corrosive environment respectively. When this ratio is less than one, the material is considered susceptible and, when this ratio is equal to one, it is said not to be susceptible [9, 22, 25]. Figure 7 shows a comparison of results obtained for the ratio of reduction of area of welded joints tested in different environments. For the more acidic test solutions, 1 and 3 (pH = 3.4), a significant reduction in ductility is shown (Figure 7). This behaviour can be attributed to both, the partial dissolution of the material and to hydrogen embrittlement, since these solutions promote the production of H_2S from $Na_2S_2O_3$ [22, 26]. According to Hutchens [27], the rate of production of hydrogen is dependent on the acidity (pH) of the system, where high concentrations of species such as CO_2 and H_2S promote a reduction in pH, increasing the acidity and consequently the risk of cracking. Hydrogen absorption into the steel was favoured by the H_2S produced from thiosulphate decomposition on the sample surface. For solutions 2 and 4 (pH = 4.4), the average RRA for the welded joints was closer to 1, presenting values of percentage reduction in area similar to those obtained in air, indicating a lower susceptibility to SSCC and hydrogen embrittlement.

JCSE The Journal of Corrosion Science and Engineering
ISSN 1466-8858 Volume 14, Preprint 43 submitted 6 December 2011

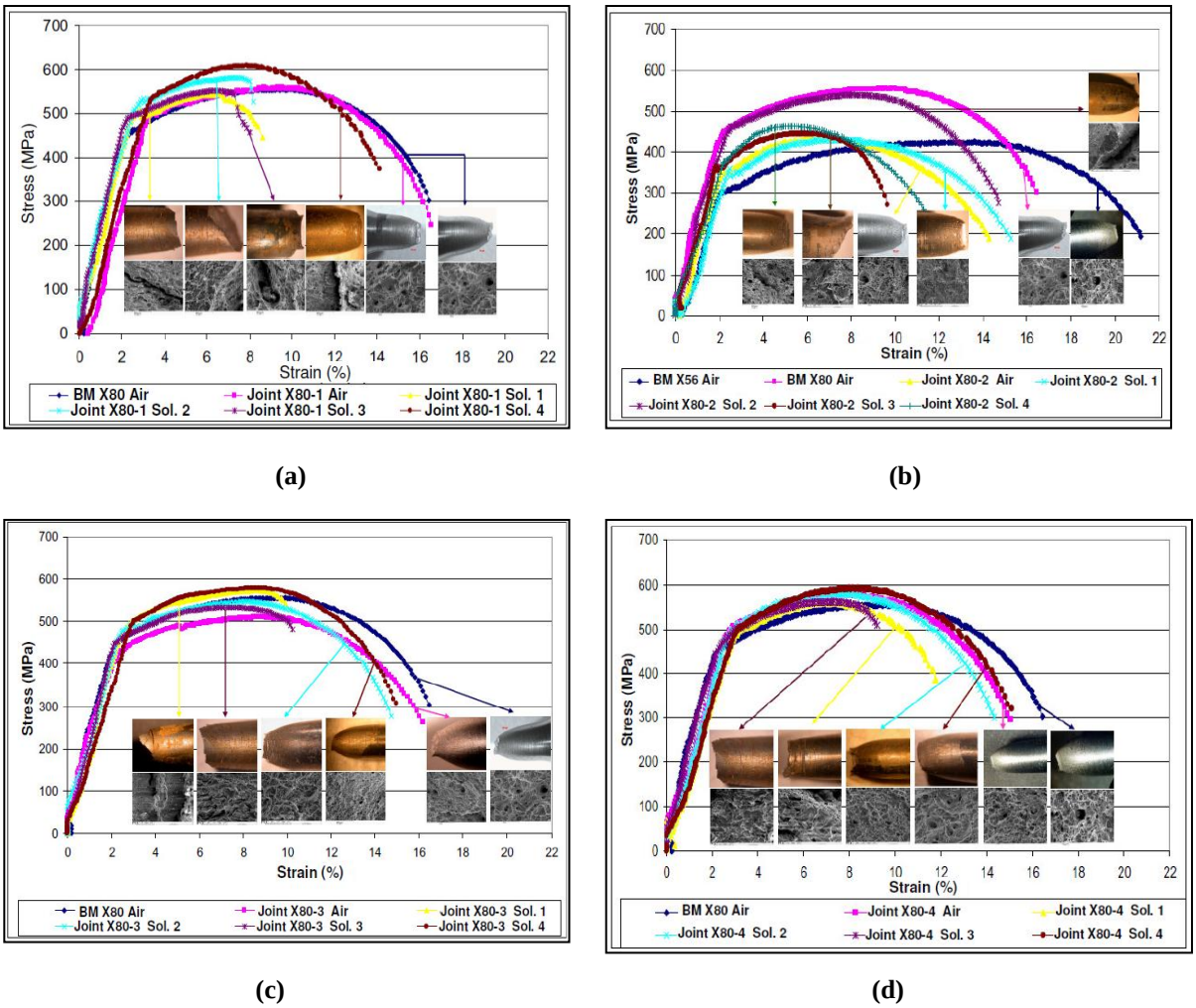

Figure 6. Stress-Strain Curves for the different environments studied. (a) Joint X80-1. (b) Joint X80-2. (c) Joint X80-3. (d) Joint X80-4

For similar joints (X80 – X80) 80% of the total specimens tested in solution fractured in the base metal, and for the dissimilar joints (X80 – X56) the fracture occurred in the lower strength (X56) base metal. Only 10% of the specimens tested in solution fractured in the weld metal; and in most cases the presence of weld defects such as porosity, lack of fusion and slag inclusions, were confirmed. It is important to point out that all these welds were approved according to the API 1104 standard recommendation. This suggests that the limiting defect size that leads to failure under SSCC conditions is different to that specified for a standard approved weld under non-SSCC conditions. Such defects act as stress concentrator elements and, potentially, traps for the accumulation of hydrogen. In a minority of cases, fracture also occurred at the fusion line (5%) or in the heat-affected zone (5%).

The SSR test results indicate that the more susceptible microstructures to hydrogen embrittlement and SSCC were those comprising ferrite-pearlite and ferrite with microconstituent MA (BM X56 and BM X80 respectively), while the least susceptible microstructures were acicular ferrite, grain boundary ferrite (weld metal) and lower bainite (HAZ). One possible explanation for this phenomenon could be associated with the fact that the acicular ferrite and bainite microstructures have a low hydrogen trapping capacity due to the presence of very fine carbides in its structure, therefore lower interfacial area between the ferrite phase and carbides.

Sakamoto [28,29] suggests that there is an increasing order of microstructural permeability where a quenched matensite microstructure is the less permeable and the coarse pearlitic microstructure would be the most permeable therefore less susceptible to hydrogen embrittlement. However according to Robertson and Thompson [30] cementite –ferrite interfaces are hydrogen traps suggesting that dislocations can be the main trapping mechanism. On another hand, Wu [31] and collaborators suggests that pearlite is more susceptible to hydrogem embrittlement than spheroidized pearlite. All these studies [28-31] where developed in steels with very high carbon content, in our case the of the base metal of steel in study it has a much lower carbon content (0.08%C) and in the case of the X80 lower dislocation density and very fine precipitation [32]. At the HAZ occurs a coarsening of the precipitates and in the case of X80 MA decomposition. These microstructural transformations may have contributed for a reduction in solubility of hydrogen at the HAZ the same didn't occur at the base metal leading to fracture. Mori et al.[33], reported that in medium and high strength steels, lower bainitic microstructure offers a low susceptibility against HE, and is less vulnerable when comparing to ferritic-perlitic, tempered-quenched martensite microestrutures. This is mainly attributed to its stress-free conditions and homogenous microstructure nature. However, there is no agreement regarding the microstructure trapping efficiency, as showed by several authors [34-38]. Another fact that can contribute to increase the resistance to SCC is the fine grain size present in these regions (acicular ferrite and bainite microstructures) [8], in terms of the rate of cracking, because it presents a greater number of obstacles to growth and the grain boundaries offer resistance to crack propagation.

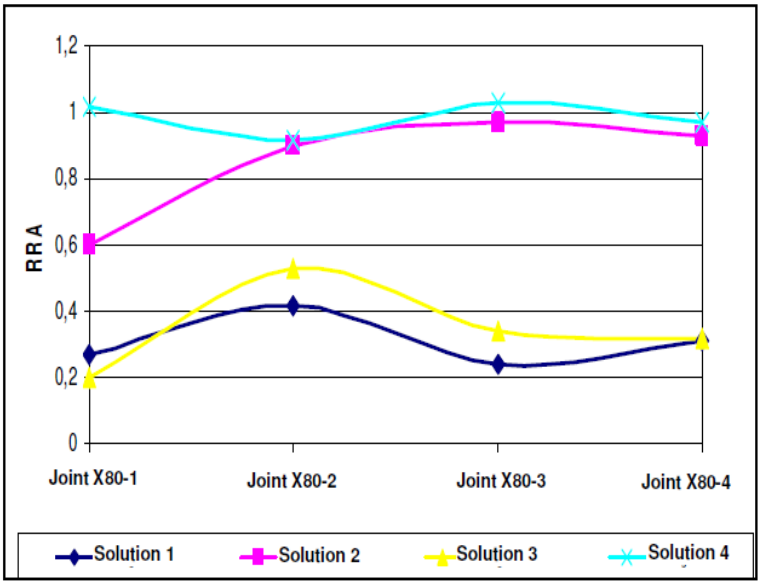

Figure 7. Comparison of the test results for the air/solution reduction in area ratio for the welded joints in each tested solution.

These results are in agreement with other studies [3, 8, 39- 43], in which it was found that lath-like and heterogeneous structures such as ferrite-pearlite are more susceptible to hydrogen embrittlement and SSCC. Bainite and acicular ferrite are considered microstructures less likely to suffer SSCC and HE. Lu [40] studied high strength low alloy steels (X52 to X100) in SSR tests, and found that steels with ferrite-bainite microstructure exhibited a greater resistance to the SCC than steels with a microstructure of ferrite-pearlite. Mign [7], worked with low carbon microalloyed steels, and compared the results for steels with a microstructure of acicular ferrite and ultrafine ferrite with steels posessing ferritic-pearlitic microstructures. This author found that the acicular ferrite and ultrafine ferrite are not susceptible to hydrogen embrittlement

and SCC, while the ferrite-pearlite microstructure was. These results coincide with the results presented in the present study.

One of the parameters used to determine if a steel is suitable for sour service in water containing H_2S, is its hardness [2, 27, 44, 45]. The NACE MR0175 [24] standard specifies that the hardness of a carbon steel and its welded joint, should not exceed a Rockwell C value of 22, equivalent to 248Hv (Vickers hardness). If this value is exceeded, the steel is considered to be susceptible to SSCC and not suitable for work in sour environments. The NACE MR0175 standard lists materials according to their resistance to SSCC, either by service experience or through laboratory testing using the NACE TM0177 standard method. The determination of this hardness limit excludes the application of many HSLA steels because after welding, these can exhibit high hardness in specific regions of the welded joint.

In this work, the base metal had an average hardness value of 242.5 HV_{10}. The HAZs obtained by the different procedures presented average hardness values of less than 248 Hv_{10}, (hardness of approximately 229.5 HV_{10}) and the weld metal an average hardness was 245.7 HV_{10} (Figure 8). Thus, according to this standard, the base metals and the welded joints would not be considered susceptible to SSCC. Nevertheless, all joints were in fact susceptible to SSCC in the more acid solutions, thus the hardness criterion specified in the standard was not valid for this case.

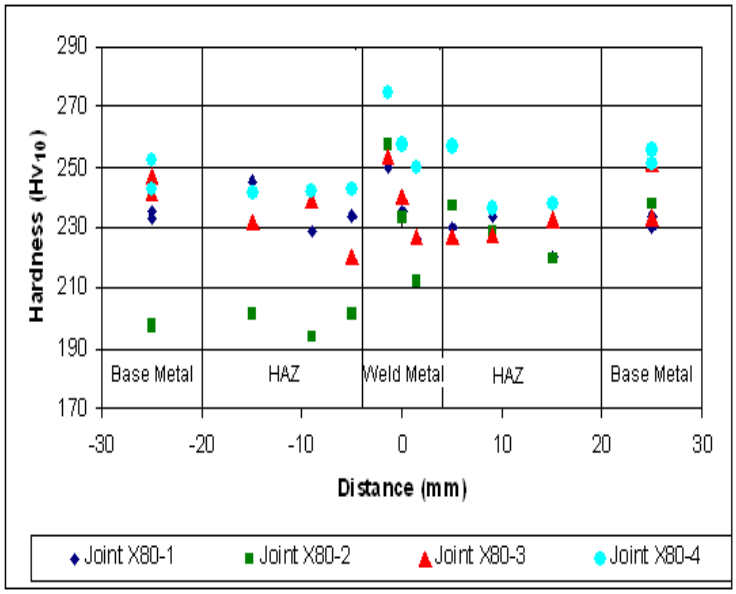

Figure 8. Hardness distributions for the welded joints.

The specimens subjected to SSR tests in solution were found to exhibit secondary cracks along the gauge lengths (Figure 9a) and internal cracks in the cross section (Figure 9b). Similar studies suggest (Lima et al [26]), that these types of crack are usually associated with the recombination of hydrogen atoms, previously in solid solution, to form hydrogen molecules at microstructural interfaces. For some tests in air, transverse cracks were observed on the surface, which were associated with delamination of the metal (Figure 9c). For specimens which had been tested in solution, in addition the presence of delamination cracks, internal transverse cracking was also observed in the form of steps, with a different morphology to the cracks observed on the delaminated surfaces. The step-like morphology internal cracking (Figure 9c) is called Chevron cracking [46] and its occurrence may be due to the retention, within the specimen, of hydrogen generated from thiosulphate decomposition on the surface metal.

JCSE The Journal of Corrosion Science and Engineering
ISSN 1466-8858 Volume 14, Preprint 43 submitted 6 December 2011

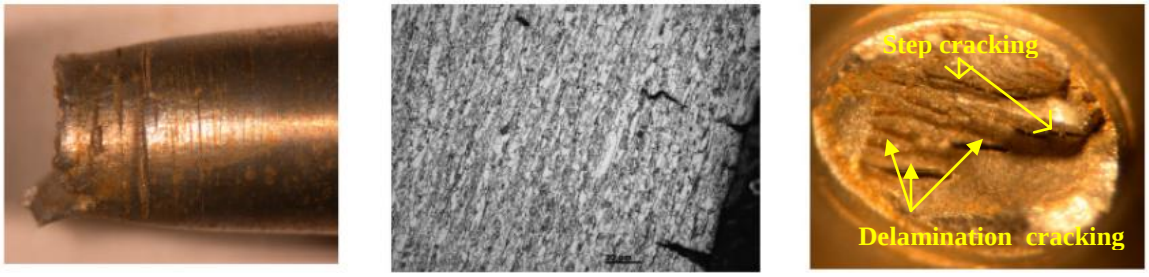

(a) **(b)** **(c)**

Figure 9. Fracture surfaces of SSR test samples. (a) Secondary cracks. (b) Internal transverse cracks. (c) Metal delamination cracks.

Cracks were also observed to have originated at points of localized attack (pitting) or in regions with defects. In these cases the crack propagation was oriented towards the interior of the grains, occurring preferentially in a transgranular form (Figure 10a). For most of the welded joints, a mixed fracture morphology was observed, featuring both brittle fracture by quasi-cleavage and ductile fracture by micro-dimples (Figure 10 b). These results were typical for all samples tested and are consistent with the results obtained by other researchers [16, 38, 47-49].

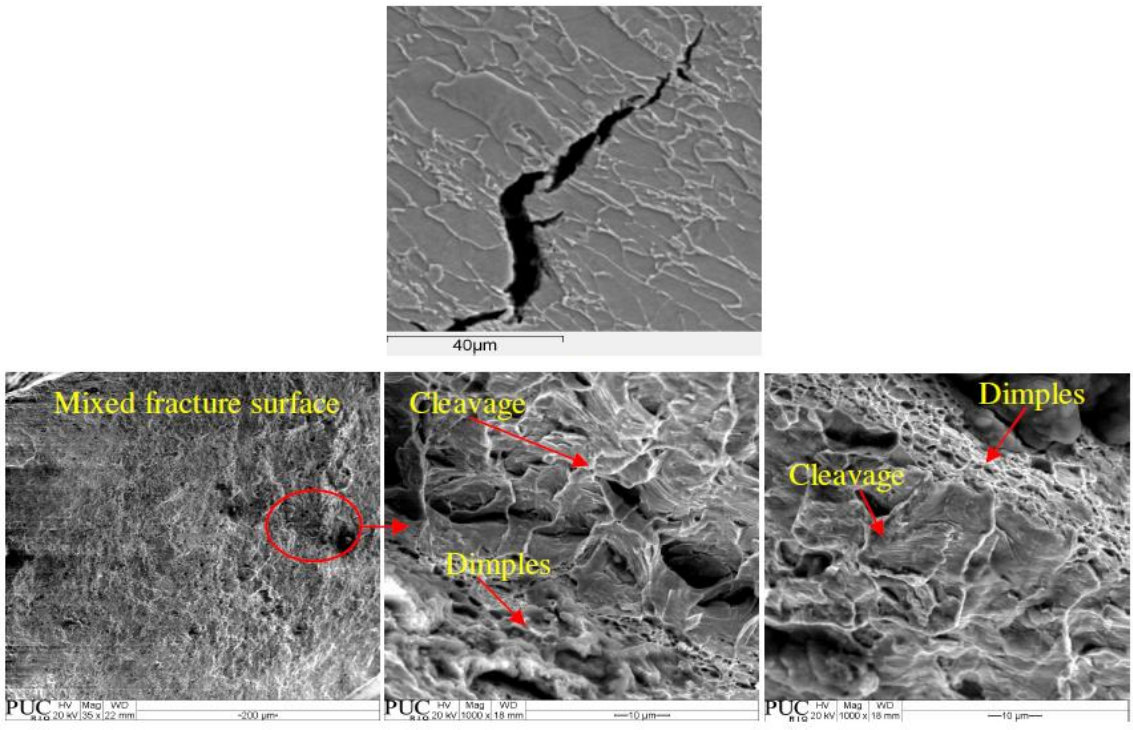

(b)

Figure 10. **(a)** Transgranular cracking observed in the SSR test specimens. **(b)** Mixed fracture surface of SSR test specimens.

3.2 Hydrogen Permeation Tests

JCSE The Journal of Corrosion Science and Engineering
ISSN 1466-8858 Volume 14, Preprint 43 submitted 6 December 2011

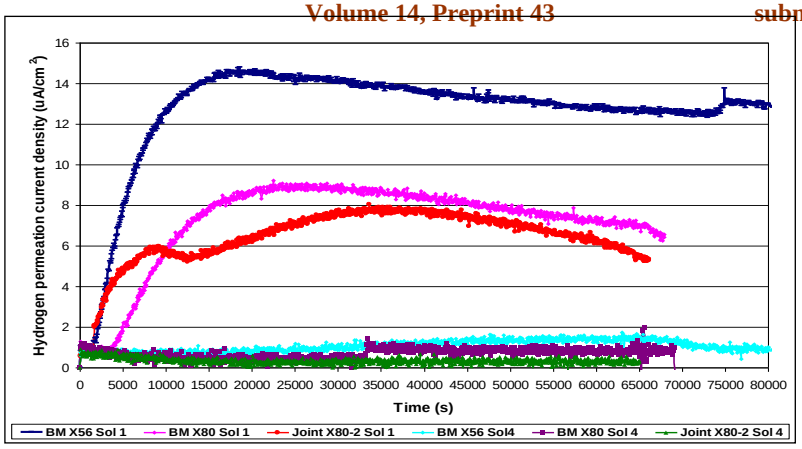

Figure 11. Hydrogen permeation curves for the dissimilar joint (X80-X56) exposed to test solutions 1 and 4

The evolution of the hydrogen permeation flux with time, (Figures 11 and 12) shows that the highest permeation current density was obtained for the two base metals; X56 (14.7μA/cm^2) with a ferrite-pearlite microstructure, and X80 (9μA/cm^2) with a ferrite-MA microstructure, and the lowest current density was obtained for the X80-3 joint (6.5μA/cm2) and X80-2 joint (7.8μA/cm^2). These results confirm that the microstructures present in the weld metal and HAZ are potentially less susceptible to stress corrosion cracking, and may also confirm that these microstructures have lower hydrogen diffusion coefficients and a greater solubility for this element.

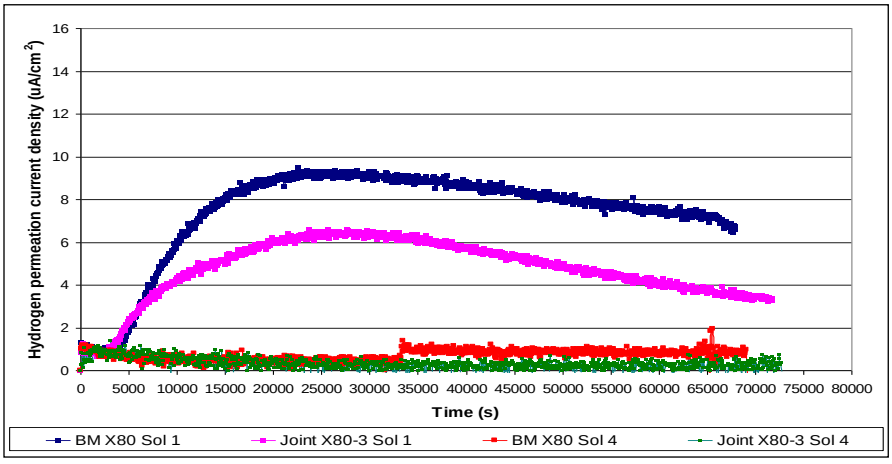

Figure 12. Hydrogen permeation curve for the similar joint (X80-X80) exposed to solutions 1 and 4

The increase in the measured current density results from the electric current associated with the oxidation of hydrogen emerging from the sample surface exposed in the anodic compartment of the test apparatus. The amount of hydrogen effectively permeating through the sample was found to be dependent on the pH and on the amount of Thiosulfate added to the cathodic compartment of the system [50]. For a pH of 3.4 and 10^{-3} mol of Thiosulfate an increase was observed in the hydrogen permeation current density with time (Figures 11 and 12). For systems with pH = 4.4 and 10^{-4} mol of Thiosulfate, by contrast, no increase in

ISSN 1466-8858 Volume 14, Preprint 43 submitted 6 December 2011

hydrogen permeation current density was observed (Figures 9 and 10), indicating that little or no permeation occurred during the testing times applied, and therefore the phenomenon of embrittlement is less likely to occur. In Silva´s studies [51], the testing conditions led to a pH lower than 7 and the hydrogen permeation rates generally increased with decreasing pH, indicating that at more acidic pH levels the corrosion densities obtained were larger, as was the case for the results obtained in the present study.

4. Conclusion

As a general trend, SSR tests showed that the majority of the welded joints tested in solutions with pH=3.4, exhibited a reduction in ductility, indicating a susceptibility to sulphide stress corrosion cracking and hydrogen embrittlement. The tests in solutions with pH = 4.4 showed similar results to the air tests, with RRA values close to 1, indicating little susceptibility to SSCC and HE. These results were consistent with hydrogen permeation test results. These permeation results revealed an increase in the hydrogen permeation current density for the base metal and welded joints in solution 1, while for solution 4, this increase did not appear. This indicates that the pH has a strong influence on the effective susceptibility of the steels under study to SSCC and HE.

The results obtained in the SSR and hydrogen permeation tests, indicate that the microstructures most susceptible to HE and SSCC are ferrite-pearlite (BM X56) and ferrite with MA microconstituent (BM X80). The least susceptible microstructures were acicular ferrite, grain boundary ferrite (weld metal) and inferior bainite (HAZ).

The evaluation of the fracture surface for samples from the SSR tests in solution revealed the presence of secondary longitudinal cracks and internal transverse cracks indicating the action of hydrogen as an embrittleming element. The predominant modes of fracture were transgranular, and a mixed fracture morphology, exhibiting both quasi-cleavage fracture and ductile fracture by micro-dimples.

The welds were approved according to the API 1104 standard recommendations, suggesting that the limiting defect size that leads to failure under SSCC condition is different to that specified for a standard approved weld.

5. Acknowledgements

The authors wish to acknowledge the financial support of CNPq, FAPERJ, CAPES and CENPES – PETROBRAS.

Bibliography

[1] Gladman T. The physical metallurgy of microalloyed steels. UK: The Institute of Materials; 1997. pp. 185–211.
[2] Collins EL, Kostic M, Lawrence T, Mackenzie R, Townley N. High strength line pipe: current and future production. Proc. Int. Conf. on Pipeline, ASME 2000, Three Park Avenue, New York, N.Y., Canada, vol. 1; 2000. pp. 185–91.
[3] Ueda, M. Omura, T. Nakamura, S. Abe, T. Nakamura, K. Nice, P.I. Martin, J.W. Development of 125 KSI grade HSLA Steel OCTG for mildly sour environments. Corrosion 2005. Paper 05089.
[4] Omweg, G.M. Frankel, G.S. Bruce, W.A. Koch, G. The Performance of Welded High-Strength Low-Alloy Steels in sour Environments. Corrosion 2002. Paper 02048
[5] Mansour A. Sulphide Stress Cracking Resistance of API-X100 High Strength Low Alloy Steel in H_2S Environments. Thesis of Master of applied science. The University Of British Columbia. November 2007.
[6] ASM Handbook, Volume 1, Properties and Selection: Irons, Steels, and High Performance Alloys. Published in 1993. ISBN 0-87170-377-7 (V.1).SAN 204-7586. Printed in the United States of America.

[7] Miglin, B.P. Skogsberg, L.A. Grimes, W.D. Sulphide Stress Cracking of low alloy steel Uniaxial tension and DCB test in modified NACE environment. Corrosion 2005. Paper No. 05086.
[8] Ming, C. Z., Yi-Ying, S., Fu, R., Ke, Y., Yu, H. Investigation on the H_2S-resistant behaviours of acicular ferrite and ultrafine ferrite. Materials Letters. No. 57. Elsevier, November 2002. pp. 141-145.
[9] Guedes, M O ; Gomes, J. A. C. P ; Payao,J . Assessment of Hydrogen Induced Damages on ASTM 516 Grade 60 Steel Welded Joints by Slow Strain Rate Tests. In: EUROCORR 2000, London. Proceedings of Eurocorr 2000. London EFC, 2000.
[10] Shenton, P.A. The Effect of Strain on the Susceptibility of Pipeline Girth Welds to Sulphide Stress Cracking. Corrosion, 2005. Paper 05117.
[11] Zhiyong L. Guoli Z. Xiaogang L. Cuiwei D. Materials. Journal of University of Science and Technology Beijing. Vol 15. No. 6. December 2008. pp. 707.
[12] Ping L. Xiaogang L. Cuiwei D. Xu Ch. Materials and Design 30 (2009). pp. 1712-1717
[13] Hulka, K. Brian, J. "High Strength Pipeline Steels for Arctic and Sour Environment Processed under Non-Severe Rolling Conditions". HSLA Steels'85 Conference. Beijing, China, 1985. pp. 475-484.
[14] Billingham, J. Sharp, J.V. Spurrier, J. Kilgallon, P.J. Review of the Performance of High Strength Steels Used Offshore. Research Report 105. Prepared by Cranfield University for the Health and Safety Executive 2003.
[15] Koch G.H. Tests for Stress Corrosion. Advanced Materials & Processes. CC Technologies Inc, Dublin, Ohio. August 2001.
[16] Moro, I. Briottet, L. Lemoine, P. Andrieu, E. Blanc, C. Odemer, G. Hydrogen embrittlement susceptibility of a high strength steel X80. Materials Science and Engineering A. 527. 2010. Pg. 7552-7260
[17] Delafosse D. Magnin T. Engineering Fracture Mechanics 68. 2001. pp. 693-729.
[18] Torres A. Gonzalez J.G. Uruchurtu J. Serna S. CORROSION Science 50 (2008). p. 2831-2839
[19] Zhang G.A, Cheng Y.F. Corrosion Science 51(2009). pp. 1714-1724.
[20] Brown, B.F. Stress Corrosion Cracking Control Measures, Chemistry Department, p. 32, Nov 1981.
[21] Leyer, J. Sutter, P. Marchebis, H. Bosch, C. Kulgemeyer, A. Orleans, J. BJ. SSC resistance of a 125 Ksi steel grade in slightly sour environments Corrosion 2005. Paper 05088.
[22] ASTM. G129-00 Standard Practice for Slow Strain Rate Testing to Evaluate the Susceptibility of Metallic Materials to Environmentally Assisted Cracking. 2006.
[23] Specification for Line Pipe, API Specification 5L. American Petroleum Institute, March. 2004.
[24] International Standard NACE MR0175/ISO15156 - Petroleum and Natural Gas Industries – Materials for use in H2S-containing Environments in Oil and Gas Production. 2001.
[25] Rocha, P. J. E. Gomes, J. A. C. P. Electrochemical Noise Characterization of Base Metal and Weld Metal of an ASTM 516 Steel in H_2S Containing Environment. Werkstoffe und Korrosion / Materials and Corrosion, Frankfurt, n. 3, pp. 201-203, 2001.
[26] Lima, K.R.S. Bott, I.S. Ponciano, J.A. Laboratory Investigation of Environmentally Induced Cracking of Api-X70 and X80 Pipelines Steels. 24TH International Conference on Offshore Mechanics and Arctic Engineering (OMAE). June, 2005.
[27] Hutchens, T. Carbon-Manganese and low alloys steels in sour service. TWI Knowledge Summary. 2007.
[28] Sakamoto, Y. Montani, T. of Quenching and Tempering on Diffusion of Hydrogen in Carbon Steel. Trans. Jpn Inst. Metals, 17. 1976. Pg. 743-748
[29]Sakamoto, Y. Takao, K. Tokumitsu, S. Effect of Quenching and Tempering on Diffusion of Hydrogen in High-Strength alloy Steels. Trans. Jpn Inst. Metals, 18. 1977. Pg. 603-609
[30] Wayne M. Robertson and Anthony W. Thompson: Metall. Trans. A, 1980, vol. llA. Pg. 553-57
[31] H. W. Jeng, L. H. Chiu, D. L. Johnson and J. K. Wu. Effect of pearlite morphology on hydrogen permeation, diffusion, and solubility in carbon steels. Metallurgical and Materials Transactions A.Volume 21 A. 1990. Pg. 3257-3259.
[32] Bott, I. S. Vieira, A. A. H. Souza, l. F. G. Rios, P. R. Microstructural Evaluation of API 5L X80 Pipeline Steels Submitted to Different Cooling Rates. Thermec, 2009, Berlin. International Conference on Processing and Manufacturing of Advanced Materials, 2009.
[33] Mori, G. Feyeri, J. Zitter, H. On the influence of hydrogen content and stress level on hydrogen embrittlement of bainitic carbon steel fasteners. Corrosion 2002, paper 02430.
[34] Arafin, M.A. Szpunar, J.A. Effect of bainitic microstructure on the susceptibility of pipeline steels to hydrogen induced cracking. Materials Science and Engineering A, 528. 2011. P 4927-4940.
[35] K.D. Chang, J.L. Gu, H.S. Fang, Z.G. Yang, B.Z. Bai, W.Z. Zhang, ISIJ Int. 41 (2001)

ISSN 1466-8858 Volume 14, Preprint 43 submitted 6 December 2011
1397–1401.
[36] G.T. Park, S.U. Koh, H.G. Jung, K.Y. Kim, Corros. Sci. 50 (2008) 1865–1871.
[37] D. Hardie, E.A. Charles, A.H. Lopez, Corros. Sci. 48 (2006) 4378–4385.
[38] F. Huang, J. Liu, Z.J. Deng, J.H. Cheng, Z.H. Lu, X.G. Li, Mater. Sci. Eng. A 527 (2010) 6997–7001.
[39] Parkins, R.N. A Review of Stress Corrosion Cracking of High Pressure Gas Pipeline, Corrosion 2000, paper 00363.
[40] Lu B. T., Luo J. L., Relationship Between Yield Strength and Near Neutral pH Stress Corrosion Cracking Resistance of Pipeline Steels- An Effect of Microstructure, Corrosion Science, 2006, vol. 62, No.2. pp. 129-140.
[41] Asahi, H. Sogo, Y. Ueno, M. Higashiyama, H. Metallurgical Factors Controlling SSC Resistance of High Strength, Low Alloy Steels. Corrosion Vol. 45, No. 6. 1989. pp. 519.
[42] Ikawa, Hi. Oshige, H. Tanoue, T. Effect of Martensite-Austenite Constituent on HAZ Toughness of High Strength Steel. July, 1980.
[43] Love, J. Ponciano, J.A. Evaluation of hydrogen embrittlement of high strength low alloy steel in thiosulphate sodium solutions. 55th ABM Congress. Rio de Janeiro. Brazil. July, 2000. (In Portuguese)
[44] Omweg, G.M. Frankel, G.S. Bruce, W.A. Ramirez, J.E. Koch, G. Effect of Welding Parameters and H2S Partial Pressure on the susceptibility of welded HSLA Steel to Sulphide Stress Cracking. Welding Research. June, 2003. pp. 136-143.
[45] Beavers, J.A. Jonson, J.T. Sutherby, R.L. "Materials Factors Influencing the Initiation of Near-Neutral pH SCC on Underground Pipelines," Proc. Int. Pipeline Conf., vol. 2 (New York, NY: ASME International, 2000). pp. 979-988.
[46]Alcântara. N. G. Effects of Hydrogen in Welded Joints. Gases in Metals and Alloys. Fundamentals and Applications in Engineering. EDC. Rio de Janeiro. 1994. (In Portuguese)
[47] Martins ; Gomes, J. A. C. P ; Bott, I. S. . SAW welded Joints of Two API Steels Subject to SCC Laboratory Testing. Materials Science Forum, v. 539. pp. 4440-4445, 2007.
[48] Bueno, A. H. ; Gomes, J. A. C. P . Environmentally induced cracking of API Grade steels in near-neutral pH soil. Journal of the Brazilian Society of Mechanical Sciences and Engineering (Impress), v. XXXI. pp. 97-104, 2009.
[49] Kim. W. Jung, H. Park, G. Koh, S. Kim, K. Relationship between hydrogen-induced cracking and type I sulphide stress cracking of high-strength linepipe steel. Scripta Materialia. 2010. pp. 195-198.
[50] Kittel, J. Smanio, V. Fregonese, M. Garnier, L. Lefebvre, X. Hydrogen induced cracking (HIC) testing of low alloy steel in sour environment: Impact of time of exposure on the extent of damage. Corrosion Science 52. 2010. pp. 1386-1392.
[51] Silva. P.R. A study of application of electrochemical technique for monitoring corrosion in fluid catalytic cracking units. (PIPE), Federal University of Parana, Curitiba. 2002.